ISSN 1027-4510, Journal of Surface Investigation: X-ray, Synchrotron and Neutron Techniques, 2021, Vol. 15, Suppl. 1, pp. S73–S80. © Pleiades Publishing, Ltd., 2021.
Russian Text © The Author(s), 2022, published in Poverkhnost', 2022, No. 3, pp. 79–88.

Splitting of the Transverse-Motion Energy Levels of Positrons during Channeling in the [100] Direction of a Silicon Crystal

V. V. Syshchenko[a], *, A. I. Tarnovsky[a], V. I. Dronik[a], and A. Yu. Isupov[b]

[a] *Belgorod State University, Belgorod, 308015 Russia*

[b] *Laboratory of High Energy Physics, Joint Institute for Nuclear Research, Dubna, 141980 Russia*

**e-mail: syshch@yandex.ru*

Received April 30, 2021; revised June 25, 2021; accepted June 30, 2021

Abstract—The motion of charged particles in the crystal can be both regular and chaotic. Within the quantum approach, chaos manifests itself in the statistical properties of the set of energy levels. The systems in which regions of regular motion are separated by that of chaotic motion in phase space are of special interest. The statistics of levels of these systems is greatly influenced by the possibility of tunneling between phase-space regions dynamically isolated from each other. Matrix elements for such tunneling transitions are estimated in the present paper. To do this, all transverse-motion energy levels of 20 GeV positrons moving in the axial-channeling mode along the Si crystal [100] direction, as well as the Hamiltonian eigenfunctions corresponding to these states, are calculated numerically. The superposition of these eigenfunctions that correspond to classical orbits localized in symmetric but dynamically isolated regions of phase space are found. The energy-level splitting makes it possible to estimate the tunneling-transition matrix elements.

Keywords: regular dynamics, chaotic dynamics, quantum chaos, channeling, semiclassical approximation, level-spacing statistics, Berry–Robnik distribution, dynamical tunneling, chaos-assisted tunneling, Podolskiy–Narimanov distribution

DOI: 10.1134/S1027451022020203

INTRODUCTION

The statistical properties of the set of energy levels of a quantum system that is chaotic in the classical limit differ sharply from those for an integrable system with regular dynamics [1–4]. This difference is due to the fact that the energy levels of the integrable system do not interact with each other, while there is the interaction of energy levels of the nonintegrable (chaotic in the classical limit) system, which leads to their mutual repulsion. The manifestations of dynamic chaos in electron channeling [5, 6] were studied in [7–11] for the case of motion near the silicon-crystal [110] direction. In this case, pairs of neighboring atomic chains create a two-well potential, above the saddle point of which the motion of electrons turns out to be almost completely chaotic. It was found that the statistical properties of the levels in this region are well described by the Wigner distribution [1–4].

The case where, at a given energy, the classical dynamics of a particle turns out to be regular under some initial conditions and chaotic under others is more complicated; in this case, the regions of regular motion are separated by the region of dynamic chaos in the phase space. Such a case is implemented, for example, when an electron moves near the silicon-crystal [100] direction [12, 13]. The authors of [14] assumed that these regions generate two independent sequences of levels. However, tunneling between dynamically isolated regions of the phase space lead to the interaction of energy levels generated by states localized in such regions. The theory that takes into account the influence of tunneling transitions on the level statistics was proposed in [15].

In this paper, we estimated the matrix elements of such transitions for the case of the channeling of high-energy positrons in the silicon-crystal [100] direction. Based on the structure of the phase space of the system established in [13], we present the interpretation of the splitting of energy levels.

EXPERIMENTAL

The motion of a relativistic particle in a crystal at a small angle to the crystallographic axis densely packed with atoms can be described as two-dimensional motion in the transverse (relative to the axis) plane under the influence of continuous potentials averaged along atomic chains, which are perpendicular to this plane, while preserving the longitudinal component of the particle momentum $p_{\|}$. The continuous potential

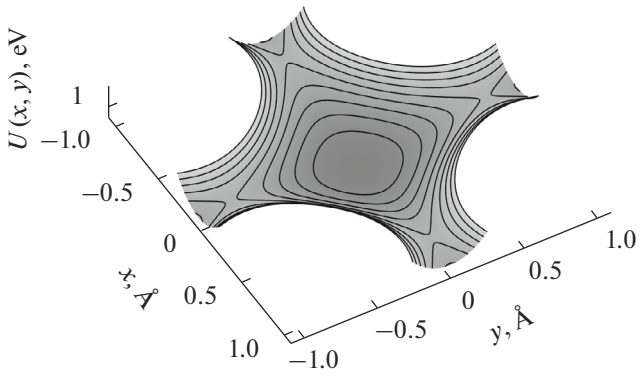

Fig. 1. Potential energy (2) of the positron moving near the silicon-crystal [100] direction.

of the separate atomic chain can be approximated by the formula [5]:

$$U_1(x,y) = U_0 \ln\left(1 + \frac{\beta R^2}{x^2 + y^2 + \alpha R^2}\right), \qquad (1)$$

where, for the silicon-crystal [100] chain, $U_0 = 66.6$ eV, $\alpha = 0.48$, $\beta = 1.5$, R = 0.194 Å (the Thomas—Fermi radius). Such chains form a square lattice with a period of a ≈ 1.92 Å in the (100) plane. For the positron, the continuous potential of the chain is repulsive, and near the center of the square, at the vertices of which there are four chains that are closest to each other, a small potential well appears (Fig. 1), in which finite motion of the positron in the transverse plane is possible; it is called axial channeling [5, 6]. If the contributions of these four chains are taken into account, the potential energy of the positron is described by the following sum:

$$\begin{aligned} U(x,y) &= U_1(x - a/2, y - a/2) \\ &+ U_1(x - a/2, y + a/2) \\ &+ U_1(x + a/2, y - a/2) \\ &+ U_1(x + a/2, y + a/2) - 7.96 \text{ eV}, \end{aligned} \qquad (2)$$

where the constant is added to make the potential vanish at the cell center.

A quantum description of axial channeling is given by the two-dimensional Schrödinger equation with the Hamiltonian:

$$\hat{H} = -\frac{\hbar^2}{2E_\parallel / c^2}\left(\frac{\partial^2}{\partial x^2} + \frac{\partial^2}{\partial y^2}\right) + U(x,y), \qquad (3)$$

where the quantity $E_\parallel / c^2$ plays the role of the particle mass and $E_\parallel = \left(m^2c^4 + p_\parallel^2 c^2\right)^{1/2}$ is the energy of longitudinal motion [5]. In this paper, we consider the channeling of positrons with an energy of $E_\parallel = 20$ GeV. The eigenvalues (energy levels of channeled positrons) and the eigenfunctions of Hamiltonian (3) were found numerically using the so-called spectral method [16], the details of which are described in [7–10] as applied to the channeling problem.

Since potential (2) has the symmetry of a square, all available states of transverse motion can be classified according to irreducible representations of the group D_4 (or C_{4v}, which is isomorphic to it, for example, [17]), depending on the type of symmetry of the wave function. This group has four one-dimensional irreducible representations denoted by A_1, A_2, B_1, B_2, and corresponding to nondegenerate energy levels and one two-dimensional representation denoted by E corresponding to doubly degenerate levels. In what follows, we will study only nondegenerate levels.

The mechanism of the interaction of energy levels was described well in [18] (Chapters 6–8) using a two-level system as an example. We recall the results of this description, following the notation used in [18]. We consider the pair of degenerate states $|1\rangle$ and $|2\rangle$ with a clear quasi-classical meaning. If the amplitude of the transition between these two states $\langle 2|\hat{H}|1\rangle$ is nonzero, $\langle 2|\hat{H}|1\rangle = V_{21} \equiv -A$, this leads to the removal of degeneracy, so that the stationary states with a certain energy are linear combinations of states $|1\rangle$ and $|2\rangle$:

$$|\mathrm{I}\rangle = \frac{|1\rangle - |2\rangle}{\sqrt{2}}, \quad |\mathrm{II}\rangle = \frac{|1\rangle + |2\rangle}{\sqrt{2}}. \qquad (4)$$

If the presence of all other states is not considered, such a two-level system can be described by the phenomenological Hamiltonian

$$\mathbf{H} = \begin{pmatrix} E & -A \\ -A & E \end{pmatrix}, \qquad (5)$$

which is diagonal in the new basis $|I\rangle, |II\rangle$:

$$\mathbf{H}' = \begin{pmatrix} E + A & 0 \\ 0 & E - A \end{pmatrix}. \qquad (6)$$

In this paper, we consider the inverse problem: using the numerically found set of stationary states, we determine the matrix elements of transitions V_{ij} between states with a clear quasi-classical meaning (which are the states corresponding to motion in dynamically isolated regions of phase space within the classical limit). For pairs of close levels, it suffices to find a matrix of transformation from the basis of stationary states $|\mathrm{I}\rangle, |\mathrm{II}\rangle$ into that of states with a simple quasi-classical meaning:

$$\begin{pmatrix} |\mathrm{I}\rangle \\ |\mathrm{II}\rangle \end{pmatrix} = \mathbf{T}\begin{pmatrix} |1\rangle \\ |2\rangle \end{pmatrix}, \qquad (7)$$

and then

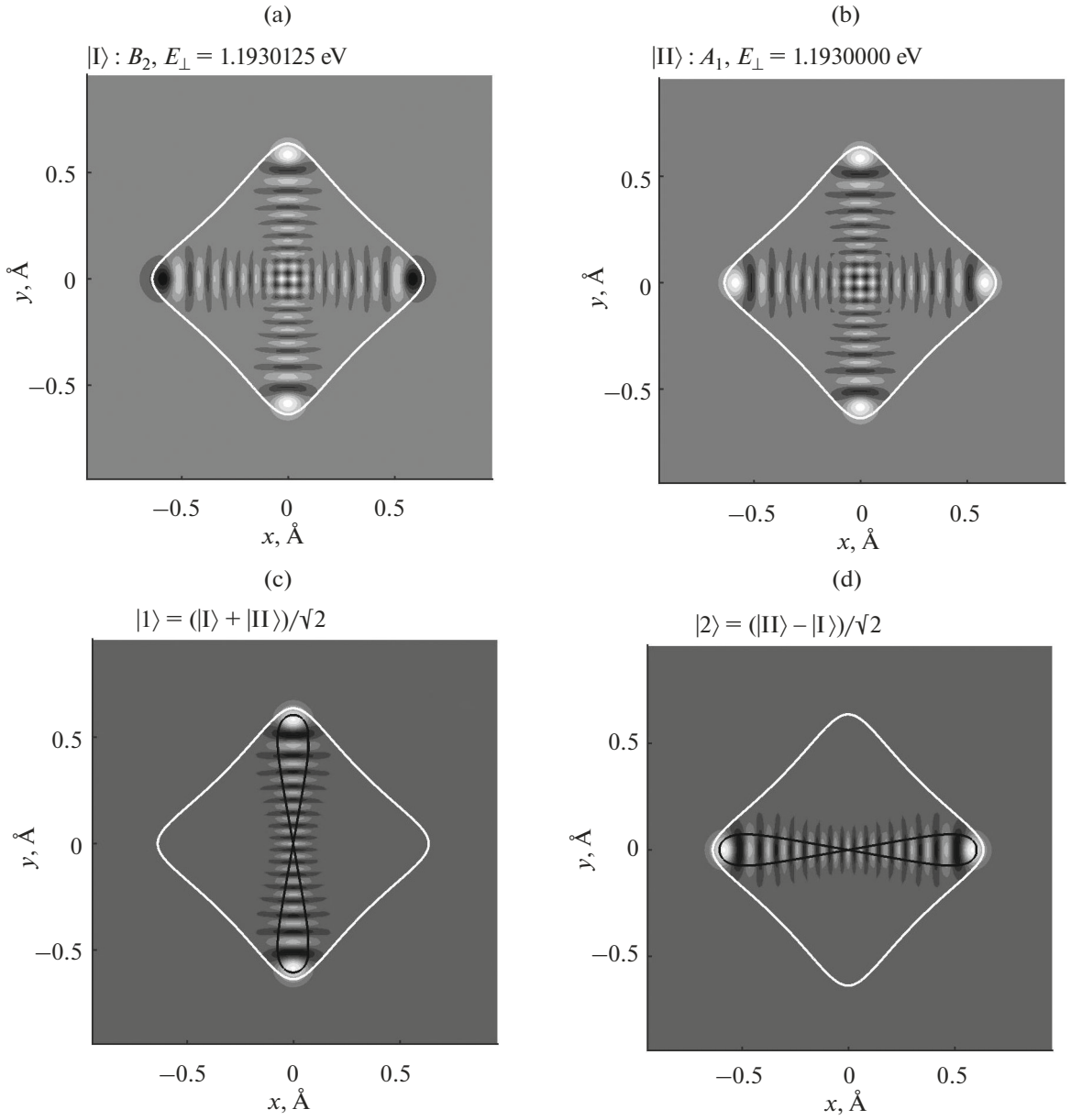

Fig. 2. Eigenfunctions of Hamiltonian (3) belonging to the representations (a) B_2 (the eigenvalue of the transverse-motion energy is $E_\perp$ = 1.1930125 eV) and (b) A_1 ($E_\perp$ = 1.1930000 eV), white lines correspond to the classical boundaries of motion; (c) and (d) superpositions (10) of these functions, black lines are the corresponding classical orbits.

$$\mathbf{H} = \mathbf{T}^{-1}\mathbf{H}'\mathbf{T}, \tag{8}$$

whence it is easy to find the sought off-diagonal matrix elements of **H**. In the above simplest case (4), the transformation matrix has the form:

$$\mathbf{T} = \frac{1}{\sqrt{2}}\begin{pmatrix} 1 & -1 \\ 1 & 1 \end{pmatrix}. \tag{9}$$

In the following section, we consider interactions of such a type and more difficult cases of the interaction of four energy levels of channeled-positron transverse motion.

RESULTS AND DISCUSSION

Among all the states of the transverse motion of positrons with an energy of $E_\parallel$ = 20 GeV, there are many pairs of states whose transverse-motion energies are close, but they belong to different representations of the symmetry group of our problem. For example, Figure 2 shows the graphs of eigenfunctions of the state with an energy of $E_\perp$ = 1.1930125 eV belonging to the representation B_2 (in our notation, this is state $|\mathrm{I}\rangle$) and of the state with an energy of $E_\perp$ = 1.1930000 eV

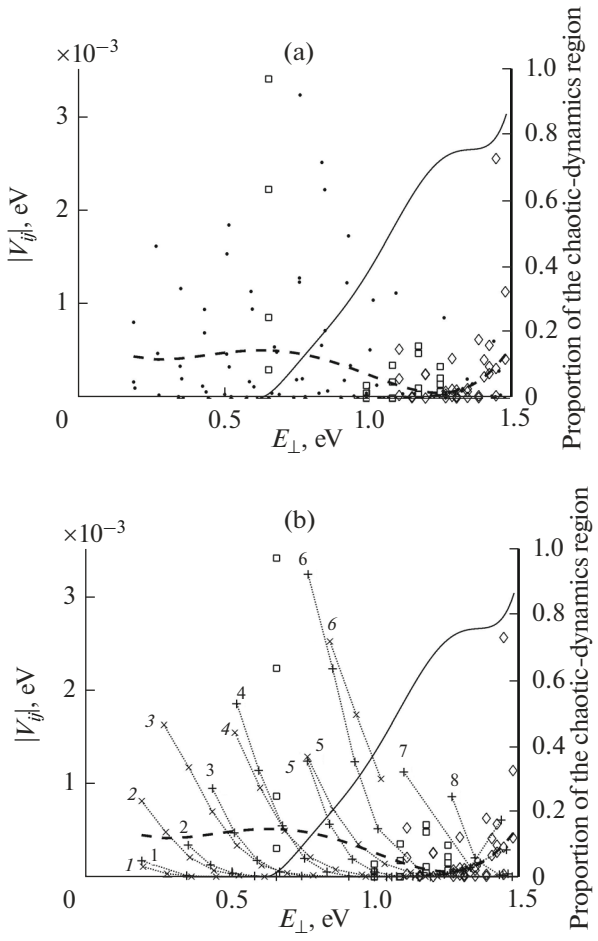

Fig. 3. (a) Absolute values of the matrix elements of the transition between quasi-classical states, the dashed line corresponds to the fitting of all found values using the fourth-degree polynomial; the solid line (the scale on the right) corresponds to the proportion of chaotic dynamics in the phase space of the system found in [13]; (b) the same with the classification of states participating in pair interactions (states belonging to the same class are connected by dotted lines).

belonging to the representation A_1 (this is state $|\mathrm{II}\rangle$ in our notation). It is not difficult to see that the combinations $|1\rangle$ and $|2\rangle$:

$$|1\rangle = \frac{|\mathrm{I}\rangle + |\mathrm{II}\rangle}{\sqrt{2}}, \quad |2\rangle = \frac{|\mathrm{II}\rangle - |\mathrm{I}\rangle}{\sqrt{2}}, \tag{10}$$

represent states localized in two dynamically isolated regions of phase space. The two curves in Figs. 2c and 2d above the graphs of wave functions show the periodic orbits realized within the classical limit at an energy of $E_\perp = (E_\mathrm{I} + E_\mathrm{II})/2$. The amplitude of the transition between these two states is immediately found from the splitting value, its absolute value is $A = (E_\mathrm{I} - E_\mathrm{II})/2 = 6.25 \times 10^{-6}$ eV. The absolute values of the transition amplitudes for all found pairs of levels are marked by points in Fig. 3a.

The regularity in the values of the transition amplitudes can be seen if we classify the states according to the number of half-waves that are located along the narrow side of the quasi-classical wave function, while separately considering the states corresponding to the classical orbits connecting two opposite corners of the potential well (such states are marked with straight crosses + in Fig. 3b) and those corresponding to orbits connecting the opposite sides of the square potential well (marked with oblique crosses ×)). For example, the states in Fig. 2 in our notation are related to the type +1. The families of states of each type are united by dotted lines in Fig. 3b.

For each of these families, the splitting value, which is dependent on the energy of the state, first decreases and then increases again. Such behavior is explained as follows. In the depth of the potential well (2), the particle dynamics is regular under almost all initial conditions, so that the boundaries of different regions of regular motion dynamically isolated from each other touch each other (Figs. 4a and 4b). Therefore, if the wave function of the state reaches the boundaries of such a region, the probability of tunnel penetration into the regular region corresponding to the partner state is rather large, which leads to a significant value of the splitting of the intrinsic energies of the symmetric and antisymmetric combinations of form (4) for these states. As the energy increases, the characteristic value of the de Broglie wavelength decreases; therefore, the state with a small number of half-waves in the transverse direction will be localized in the phase space in a region with a smaller relative volume surrounded by regions of other regular-state localization. Therefore, the probability of tunneling through dynamically inaccessible regions decreases, which leads to a decrease in the value of splitting of the corresponding energy levels. However, as the energy continues to increase, the proportion of the phase volume corresponding to regular dynamics decreases (the solid curve in Fig. 3 shows an increasing proportion of the chaotic-dynamics region). So, near the upper edge of the potential well, the phase space contains several regions dynamically isolated from each other and corresponding to different types of regular orbits separated by the region of chaotic dynamics (Figs. 4b and 4d). Therefore, wave functions of the selected type can again differ significantly from zero near the boundaries of the regions of regular motion. And although the width of the region that is dynamically inaccessible to particle motion is large, the probability of tunneling through it begins to increase because of the mechanism known as chaos-assisted tunneling [15, 19–21]. In this case, the particle only needs to penetrate beyond its dynami-

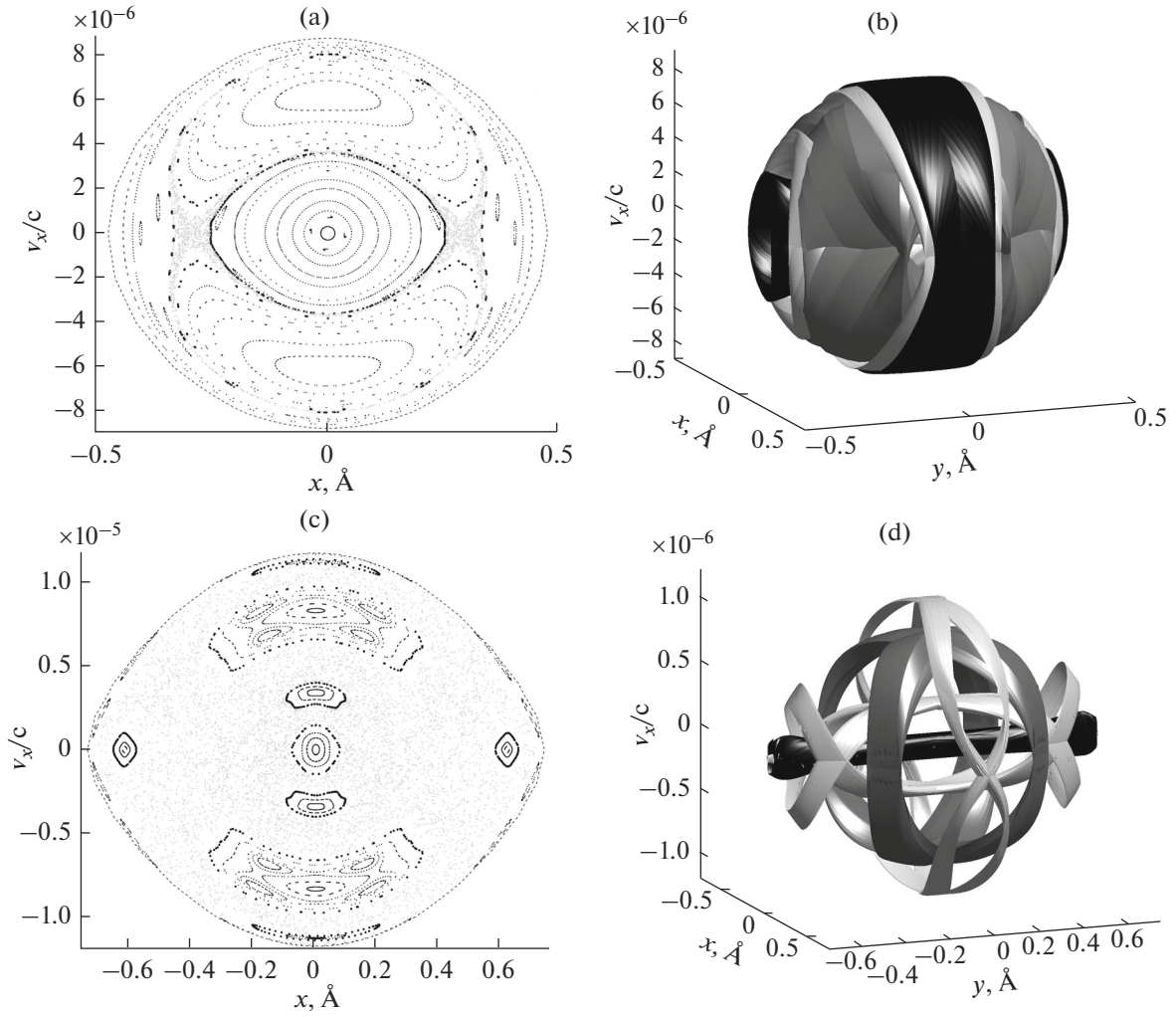

Fig. 4. (a) and (c) are the Poincare cross sections and (b) and (d) are the projections of the four-dimensional regular-dynamics regions in phase space on the half-space (x, y, v_x) for the transverse-motion energies (a), (b) $E_\perp = 0.7687125$ eV and (c), (d) $E_\perp = 1.386475$ eV.

cally allowed region, and it will be picked up by a chaotic flow, which takes it to the border of the partner region sooner or later, where the particle will be able to successfully complete the tunneling process. This is the reason for the increase in level splitting near the well top.

In addition to the numerous cases of paired interaction of levels discussed above, we found twelve cases where four energy levels corresponding to three types of symmetry interact with each other; for one of these cases, the wave functions of stationary states are shown in Fig. 5. Here, it turns out to be possible to construct combinations from two states belonging to the same type of symmetry $|\mathrm{III}\rangle, |\mathrm{IV}\rangle$, (Fig. 6):

$$\begin{aligned} |a\rangle &= \cos\alpha|\mathrm{III}\rangle - \sin\alpha|\mathrm{IV}\rangle, \\ |b\rangle &= \sin\alpha|\mathrm{III}\rangle + \cos\alpha|\mathrm{IV}\rangle, \end{aligned} \tag{11}$$

which are paired with the states $|\mathrm{I}\rangle$ and $|\mathrm{II}\rangle$. If this is taken into account, it is easy to generalize (7) to the case of four basis states:

$$\begin{pmatrix} |\mathrm{I}\rangle \\ |\mathrm{II}\rangle \\ |\mathrm{III}\rangle \\ |\mathrm{IV}\rangle \end{pmatrix} = \mathbf{T}\begin{pmatrix} |1\rangle \\ |2\rangle \\ |3\rangle \\ |4\rangle \end{pmatrix}, \tag{12}$$

where the transformation matrix has the form

$$\mathbf{T} = \frac{1}{\sqrt{2}}\begin{pmatrix} 1 & 1 & 0 & 0 \\ 0 & 0 & 1 & 1 \\ \cos\alpha & -\cos\alpha & \sin\alpha & -\sin\alpha \\ -\sin\alpha & \sin\alpha & \cos\alpha & -\cos\alpha \end{pmatrix}. \tag{13}$$

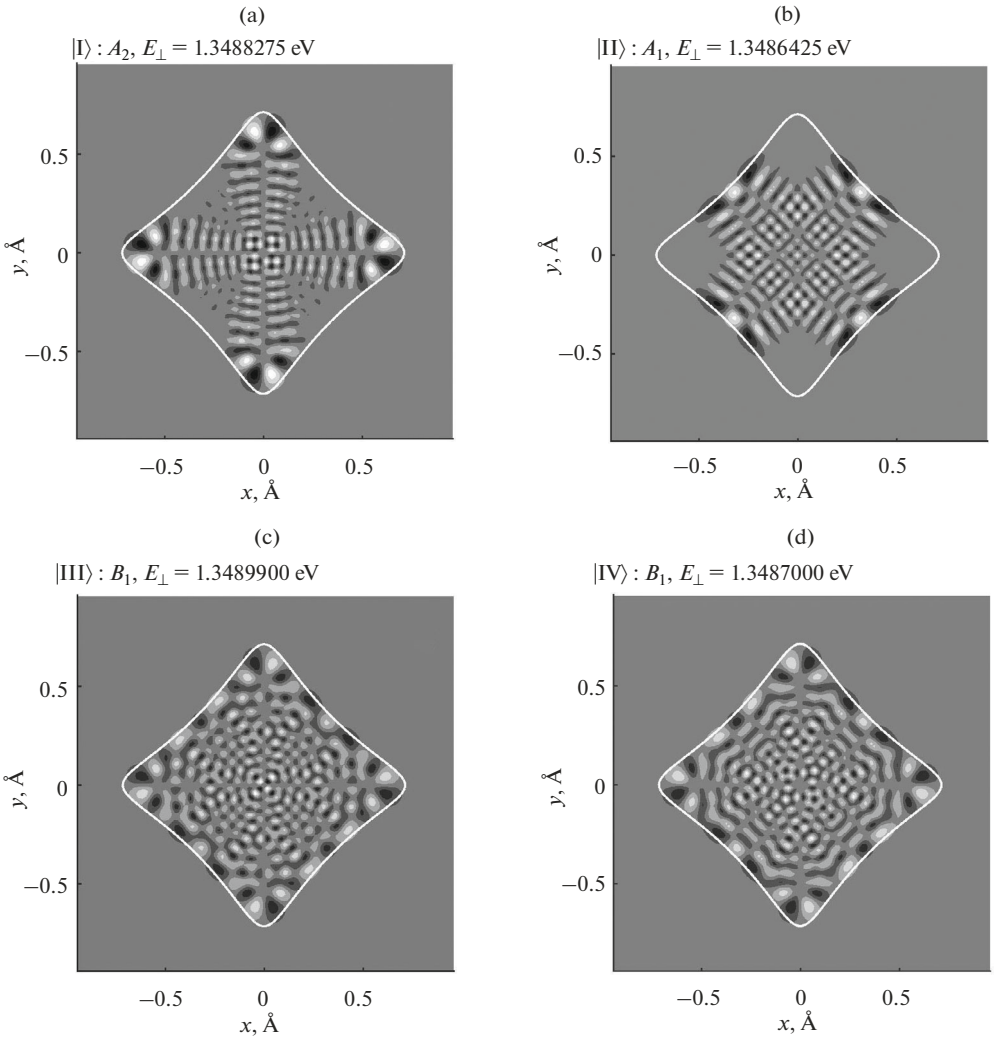

Fig. 5. Four eigenfunctions of Hamiltonian (3) belonging to three representations of the symmetry group of the problem with close eigenvalues of the transverse-motion energy.

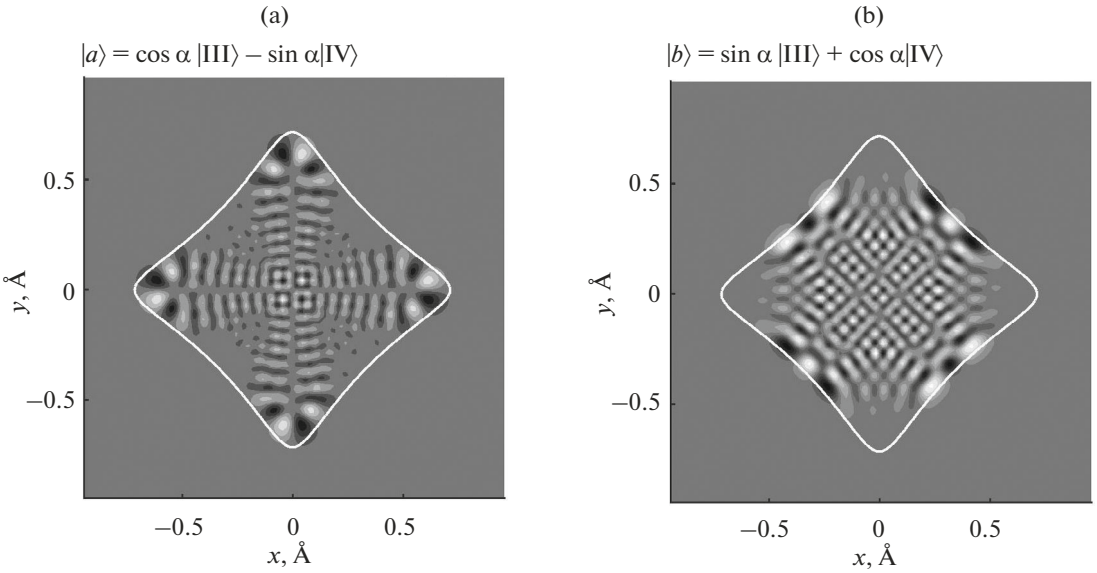

Fig. 6. Superpositions of form (11) of the functions shown in Figs. 5c and 5d. In this case, the mixing angle is $\alpha = 45°$.

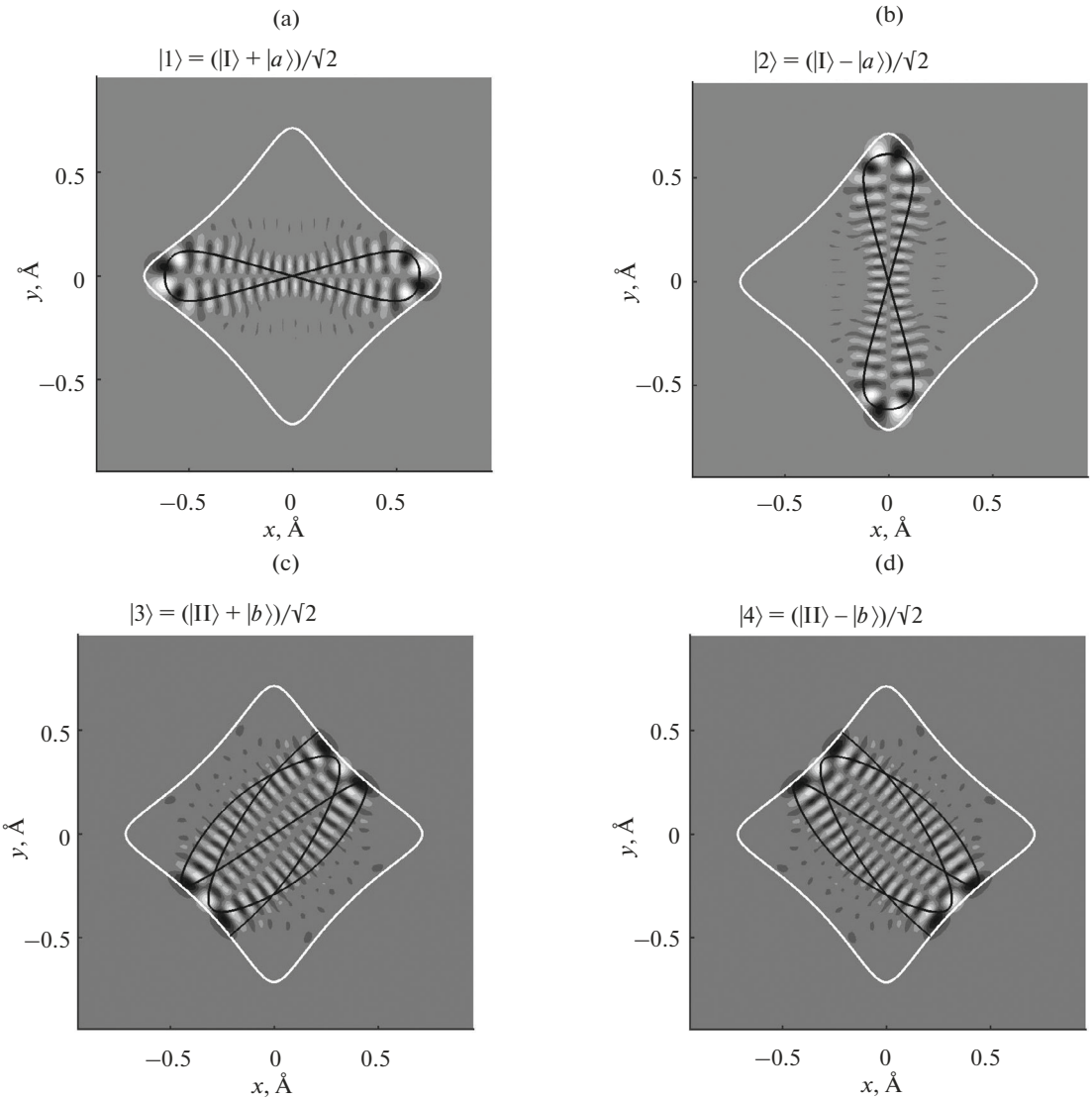

Fig. 7. Superpositions of four functions shown in Figs. 5a, 5b and 6a, 6b defined by relation (12) and the corresponding classical orbits.

The graphs of the wave functions of the states $|1\rangle$, ..., $|4\rangle$ and their corresponding classical periodic orbits are shown in Fig. 7. The values of the off-diagonal matrix elements of the Hamiltonian found after transformation (8) taking into account (13) are marked with diamonds in Fig. 3.

There are also four cases where two pairs of levels belonging to two types of symmetry interact with each other. For them, the transformation matrix is determined by two mixing angles between the states forming pairs of the same type of symmetry:

$$\mathbf{T} = \frac{1}{\sqrt{2}}\begin{pmatrix} \cos\beta & -\sin\beta & \cos\alpha & -\sin\alpha \\ \cos\beta & -\sin\beta & -\cos\alpha & \sin\alpha \\ \sin\beta & \cos\beta & \sin\alpha & \cos\alpha \\ \sin\beta & \cos\beta & -\sin\alpha & -\cos\alpha \end{pmatrix}. \qquad (14)$$

The corresponding values of the off-diagonal matrix elements of the Hamiltonian are denoted by squares in Fig. 3.

Figure 8 shows the distribution of the found nonzero values of the off-diagonal matrix elements of the Hamiltonian describing transitions between different states corresponding to dynamically isolated classical trajectories of the channeled positron (for the set of levels with $E_\perp \geq 1$ eV, for which the proportion of the chaotic-dynamics region in the phase space is significant). The standard deviation of these values is 4.2×10^{-4} eV. The square root of this value appears as a parameter in the Podolskiy–Narimanov distribution [15], which describes the statistics of interlevel distances of a quantum system, the classical analogue of which contains, in its phase space, several regular regions separated by the region of chaotic dynamics.

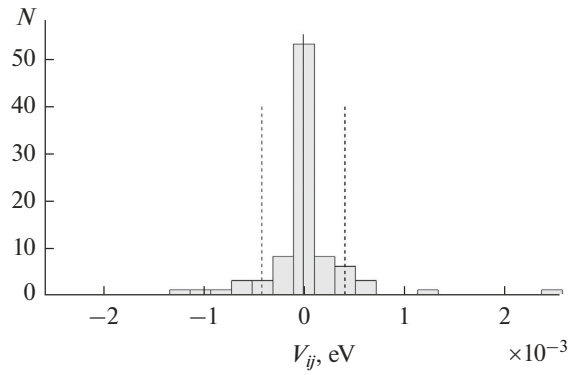

Fig. 8. Distribution of the found values of the nonzero off-diagonal matrix elements of the Hamiltonian for the set of levels with $E_\perp > 1$ eV. The dashed lines correspond to a root-mean-square deviation of 4.2×10^{-4} eV.

CONCLUSIONS

We have considered the channeling of positrons with an energy of 20 GeV near the silicon-crystal [100] direction. Numerical methods have been used to find all the energy levels of the transverse motion of positrons and their corresponding wave functions. Among these stationary states, we selected groups that can be interpreted as a result of the interaction of quasi-classical states corresponding to localization of the particle in dynamically isolated regions of phase space. We found the values of the matrix elements of the transitions between such quasi-classical states.

It is shown that near the upper edge of the potential well, the phase space contains several dynamically isolated regions corresponding to different types of regular orbits separated by a region of chaotic dynamics. In accordance with the concept of chaos-assisted tunneling (CAT), the presence of this chaotic region contributes to tunneling of the particle between regular-motion regions dynamically isolated from each other, which leads to an increase in the splitting of the energy levels of the transverse motion of channeled positrons. The found matrix elements of the transitions are consistent with this interpretation.

The obtained results (in particular, the value of the root-mean-square deviation for the set of matrix elements of tunneling transitions) can be used for statistical analysis of the interlevel distances of the quantum system under consideration within the framework of the theory of quantum chaos.

CONFLICT OF INTEREST

We declare that we have no conflicts of interest.

REFERENCES

1. M. V. Berry, Proc. R. Soc. A **413**, 183 (1987). https://doi.org/10.1098/rspa.1987.0109
2. O. Bohigas and M.-J. Giannoni, Math. Comput. Methods Nucl. Phys. **209**, 1 (1984). https://doi.org/10.1007/3-540-13392-5_1
3. H.-J. Stöckmann, Quantum Chaos (Cambridge Univ. Press, Cambridge, 2000; Fizmatlit, Moscow, 2004).
4. L. E. Reichl, *The Transition to Chaos: Conservative Classical Systems and Quantum Manifestations*, 2nd ed. (Springer, New York, 2004; RKhD, Moscow, 2008).
5. A. I. Akhiezer and N. F. Shul'ga, *High Energy Electrodynamics in Matter* (Nauka, Moscow, 1993) [in Russian].
6. A. I. Akhiezer, N. F. Shul'ga, V. I. Truten', A. A. Grinenko, and V. V. Syshchenko, Phys.—Usp. **38**, 1119 (1995). https://doi.org/10.1070/PU1995v038n10ABEH000114
7. N. F. Shul'ga, V. V. Syshchenko, and V. S. Neryabova, J. Surf. Invest.: X-ray, Synchrotron Neutron Tech. **10**, 458 (2016). https://doi.org/10.1134/S102745101602035X
8. N. F. Shul'ga, V. V. Syshchenko, A. I. Tarnovskii, and A. Yu. Isupov, J. Surf. Invest.: X-ray, Synchrotron Neutron Tech. **9**, 721 (2015). https://doi.org/10.1134/S1027451015040199
9. N. F. Shul'ga, V. V. Syshchenko, A. I. Tarnovsky, and A. Yu. Isupov, Nucl. Instrum. Methods Phys. Res., Sect. B **370**, 1 (2016). https://doi.org/10.1016/j.nimb.2015.12.040
10. N. F. Shul'ga, V. V. Syshchenko, A. I. Tarnovsky, and A. Yu. Isupov, J. Phys.: Conf. Ser., **732**, 012028 (2016). https://doi.org/10.1088/1742-6596/732/1/012028
11. V. V. Syshchenko and A. I. Tarnovsky, J. Surf. Invest.: X-ray, Synchrotron Neutron Tech. **15**, 728 (2021). https://doi.org/10.1134/S1027451021040200
12. V. V. Syshchenko, A. I. Tarnovsky, A. Yu. Isupov, and I. I. Solovyev, J. Surf. Invest.: X-ray, Synchrotron Neutron Tech. **14**, 306 (2021). https://doi.org/10.1134/S1027451020020354
13. N. F. Shul'ga, V. V. Syshchenko, A. I. Tarnovsky, V. I. Dronik, and A. Yu. Isupov, J. Instrum. **14**, C12022 (2019). https://doi.org/10.1088/1748-0221/14/12/C12022
14. M. V. Berry and M. Robnik, J. Phys. A: Math. Gen. **17**, 2413 (1984). https://doi.org/10.1088/0305-4470/17/12/013
15. V. A. Podolskiy and E. E. Narimanov, Phys. Lett. A **362**, 412 (2007). https://doi.org/10.1016/j.physleta.2006.10.065
16. M. D. Feit, J. A. Fleck, Jr., and A. Steiger, J. Comput. Phys. **47**, 412 (1982). https://doi.org/10.1016/0021-9991(82)90091-2
17. L. D. Landau and E. M. Lifshits, *Theoretical Physics*, Vol. 3: *Quantum Mechanics. Nonrelativistic Theory* (Fizmatlit, Moscow, 2016).
18. R. P. Feynman, R. B. Leighton, and M. Sands, *The Feynman Lectures on Physics* (Addison-Wesley, Reading, MA, 1964, Vol. 3; Mir, Moscow, 1966, Vol. 8).
19. O. Bohigas, S. Tomsovic, and D. Ullmo, Phys. Rep. **223** (2), 43 (1993). https://doi.org/10.1016/0370-1573(93)90109-Q
20. V. A. Podolskiy and E. E. Narimanov, Phys. Rev. Lett. **91**, 263601 (2003). https://doi.org/10.1103/PhysRevLett.91.263601
21. Y. Bolotin, A. Tur, and V. Yanovsky, *Chaos: Concepts, Control and Constructive Use* (Springer, Cham, 2017). https://doi.org/10.1007/978-3-319-42496-5

Translated by L. Kulman